Solar Active Region Evolution: Comparing Models with Observations
ASP Conference Series, Vol. 68, 1994
K. S. Balasubramaniam and George W. Simon (eds.)

Coronal Structures in Active Regions: Quantitative Results from Multi-Wavelength Observations and Comparisons with Models

Gordon D. Holman
NASA/Goddard Space Flight Center,
Code 682.1, Greenbelt, MD 20771, USA

Abstract. Microwave observations are now providing reliable determinations of the magnetic field strength in the solar corona and transition region. When combined with soft x-ray or EUV images and spectral data, these observations provide a wealth of quantitative information about the magnetic and plasma properties of active region structures. Essential to obtaining the full value from these data is the comparison of the observational results with theoretical models for the microwave and soft x-ray (or EUV) emissions, and with extrapolations of measurements of the photospheric magnetic field into the corona. I review the status of this work, and demonstrate how the combination of these multi-wavelength data and theoretical models has led to the determination of coronal magnetic field strengths and structures, plasma parameters crucial to coronal heating and particle transport theories, information about the thermal structure of the plasma at coronal heights, and tests of field extrapolations from photospheric data.

1. Introduction

One of the most intriguing aspects of the Sun is the fact that the solar atmosphere is not simply laminar and cooler than the photosphere, as expected from basic stellar models, but is made up of hot, changing structures. These coronal structures form and evolve as the Sun's magnetic field is dragged around by plasma flows near and below the photosphere. The important details of the physical properties of these magnetic structures, their evolution, and, in particular, the mechanism through which they are heated, have not been established, however. A comparison of the properties and evolution of the magnetic field and plasma in the photosphere with the properties and evolution of the magnetic field and plasma in the corona is essential to obtaining an understanding of these phenomena.

Coronal structures are most apparent in active regions. Optical observations show the structure and evolution of active regions in the photosphere. x-ray, EUV, and radio observations, on the other hand, show their coronal structure. In order to obtain a better understanding of the coupling between the photosphere, where the thermal pressure of the plasma dominates the magnetic field pressure, and the corona, where the magnetic pressure dominates the plasma pressure, it

is important to obtain simultaneous observations of photospheric and coronal structures and their evolution.

Optical observations of photospheric structures, flows, and magnetic fields are now being obtained at high spatial resolution (~1 arcsecond or better). Zeeman-effect measurements of the total vector magnetic field in the photosphere have become more available and reliable. The *Yohkoh* Soft X-ray Telescope (SXT) is providing daily images of the corona with good spatial resolution (~3 arcseconds) in at least two energy channels so that the temperature and emission measure of the x-ray-emitting plasma can be determined. Radio observations covering a broad range of frequencies and spatial scales are now available with the VLA and the Owens Valley Radio Observatory. Additional soft x-ray and EUV observations of the corona are available from occasional rocket flights. The co-registration, co-analysis, and interpretation of these diverse data sets require substantial time and effort on the part of many scientists. Such a team effort is necessary, however, in order to obtain the knowledge required to understand the coupling between the dynamic photosphere and the hot corona.

Radio observations, in addition to providing a different view of the corona from that provided by soft x-ray observations, are uniquely capable of yielding measurements of the coronal magnetic field strength. This quantitative information is especially valuable for comparison with theoretical extrapolations of the photospheric magnetic field into the corona. Such a comparison provides a test of extrapolation models, as well as of the photospheric and coronal field measurements.

Obtaining co-spatial measurements of physical quantities that describe both the plasma and the magnetic field in the solar atmosphere is crucial to assessing models for coronal heating. Models that invoke heating by magnetohydrodynamic (MHD) waves, for example, are sensitive to the value of the Alfven speed and its variation within coronal loops. In general, assessing the importance of MHD or plasma kinetic processes that may occur in the solar atmosphere depends upon having a good knowledge of these quantities.

In this paper I will demonstrate how radio observations combined with soft x-ray or EUV observations of the corona, and optical observations of the photosphere, have been used to determine the magnetic field strength and other physical quantities in the solar atmosphere. Radio emission from the low corona, corresponding to the bright loops observed in soft x-rays, is primarily observed at microwave frequencies (above 1 GHz). Two radiation mechanisms can contribute to this emission. In Section 2 I review these mechanisms and demonstrate how each can be used to determine the magnetic field strength in the corona. In Section 3 a dipole loop model is used to demonstrate how a coronal loop may appear at microwave frequencies. Examples of the application of these methods to active region data are presented in Section 4. An additional method of constraining physical parameters in the corona, making use of the propagation characteristics of the microwave emission, is also described. These results, and the future of such studies, are discussed in Section 5.

2. The Emission Mechanisms

Microwave emission from the Sun is observed to be either right- or left-hand circularly polarized, or unpolarized. The emitted radiation is in general elliptically polarized, but Faraday depolarization within the source destroys any linear component and, therefore, the radiation that leaves the source region is circularly polarized, as observed. The emissivity is greatest in the mode for which the electric field vector of the radiation rotates in the same sense as an electron around the ambient magnetic field, the *extraordinary* mode. The electric field vector rotates in the opposite direction for the *ordinary* mode. Therefore extraordinary mode emission will be right-hand polarized if the longitudinal component of the magnetic field (the component along the line of sight) is positive (pointing toward the observer), and left-hand polarized if the longitudinal component of the magnetic field is negative. The opposite polarizations would be obtained for ordinary mode emission. When the observed polarization is compared with the sign of the longitudinal magnetic field in the photosphere, the result is usually, but not always, consistent with extraordinary mode polarization.

A convenient quantity for expressing the intensity of a radio source is *brightness temperature.* Brightness temperature is defined in terms of the radio frequency (f), flux (F_f), and source area (Ω, in steradians) through the Rayleigh-Jeans Law:

$$F_f^{X,O} = kT_B^{X,O} f^2 \Omega / c^2 \qquad \text{erg s}^{-1}\ cm^{-2}\ Hz^{-1}. \tag{1}$$

X and O refer to the extraordinary and ordinary modes of polarization. Brightness temperature is a particularly useful measure of the radio flux per unit area from a thermal source, since for a uniform, isothermal plasma,

$$T_B^{X,O} = T_e(1 - e^{-\tau^{X,O}}), \tag{2}$$

where T_e is the electron temperature and τ is the optical depth of the plasma. When the plasma is fully optically thick ($\tau >> 1$), $T_B = T_e$. Therefore, the brightness temperature provides a measure of the electron temperature, or a lower limit on it.

Two emission mechanisms can contribute to the microwave radiation: *thermal bremsstrahlung* (free-free radiation) and *gyroresonance* (cyclotron) *radiation.* Nonthermal emission, such as the gyrosynchrotron radiation observed during flares, may sometimes be observable from nonflaring active regions. One indication of nonthermal emission would be an unusually high brightness temperature (greater than thermal temperatures). Other indications may be rapid time variability, or simply an inability to explain the observations in terms of thermal emission. Although there is evidence for nonthermal microwave emission from active regions that are not flaring, especially complex regions (cf. Gelfreikh 1991), it is usually not evident in observations of the relatively quiescent emission from active regions.

The optical depth to thermal bremsstrahlung is

$$\tau_{tb}^{X,O} = 9.8 \times 10^{-3} \frac{EM}{f^2 T_e^{3/2}} \ln\left(\frac{4.7 \times 10^{10} T_e}{f}\right) \cdot \frac{1}{n_f^{X,O}(1 \mp \frac{f_c}{f}\cos\theta)^2}, \tag{3}$$

where EM is the column emission measure ($\int n_e^2 dl$), $n_f^{X,O}$ is the index of refraction of the plasma (usually $\approx$1), $f_c = 2.8 \times 10^6 B$ is the electron gyrofrequency,

and θ is the angle between the direction of propagation of the radiation and the magnetic field. The upper (−) sign in the last term is for extraordinary mode emission, and the lower (+) sign is for ordinary mode. The total microwave intensity, $T_B^I = (T_B^X + T_B^O)/2$, is not very sensitive to the polarization dependent terms. Since temperature and emission measure can both be derived from soft x-ray or EUV observations of the corona, the contribution to the microwave emission of thermal bremsstrahlung radiation from plasma observed by these instruments can be determined.

The thermal bremsstrahlung polarization can be used to determine the longitudinal component of the magnetic field in the corona. The fractional polarization is, in general, $p = (T_B^X - T_B^O)/(T_B^X + T_B^O)$. When the plasma is fully optically thin and the field strength is low, $p \simeq 2(f_c/f)\cos\theta$, or

$$B_{\|}(\text{Gauss}) \simeq 179 f(\text{GHz}) \cdot p \qquad \text{when } \tau_{tb}^{X,O} << 1 \quad \text{and} \quad f_c \cos\theta << f. \tag{4}$$

Under these circumstances the value of $B_{\|}$ depends only upon the radio polarization, and not the temperature and emission measure of the plasma. Thermal bremsstrahlung often dominates at microwave frequencies below 3 GHz (cf. Gary and Hurford 1987). The optical depth of the x-ray emitting plasma is often found to be ~1 at these frequencies, however (e. g., Webb et al. 1987, Schmelz et al. 1992). The deduced value of $B_{\|}$ does then depend upon the temperature and emission measure of the plasma, and is higher than the value given by Equation 4.

Gyroresonance radiation is emitted at harmonics of the electron gyrofrequency. The magnetic field strength in the emitting region is therefore given by $f = sf_c$, or

$$B(\text{Gauss}) = 357 f(\text{GHz})/s, \tag{5}$$

where s is the harmonic number. For coronal conditions, s will generally be 2, 3, or 4. The optical depth to gyroresonance emission is approximately

$$\tau_{gr}^{X,O} \approx 0.05 \frac{s^{2s}}{2^{s+1} s!} n_e L_B f^{-1} (1.8 \times 10^{-10} T_e)^{s-1} (1 \pm \cos\theta)^2 \sin^{2s-2}\theta. \tag{6}$$

While the optical depth to thermal bremsstrahlung depends upon the plasma emission measure, the optical depth to gyroresonance emission depends linearly upon the electron density, n_e, and the magnetic scale length, L_B. Determining the harmonic number is largely a matter of obtaining constraints upon $n_e L_B$. The harmonic number is also constrained by the observed polarization. As a rule of thumb, the highest optically thick harmonic in the corona is the 3rd in the extraordinary mode, and the 2nd in the ordinary mode (e. g., Zheleznyakov 1965). When the harmonic cannot be uniquely determined, assuming the emission to be 4th harmonic puts a lower limit on the field strength that will generally be within a factor of 2 of the correct value.

Thermal gyroresonance emission is sharply peaked around each harmonic. For coronal temperatures, the range of magnetic field strengths that will contribute significantly to the emission from a given harmonic is limited to $\Delta B \leq 0.1 B_{\|}$. Likewise, the thickness of the layer contributing to the emission is $\Delta L \leq (0.1\cos\theta) L_B$. Therefore, the emission at a given radio frequency arises from a narrow range of magnetic field strengths within a relatively thin layer of the source region. Observations at another radio frequency will detect a different part of the source.

3. A Coronal Loop Model

Computations of the microwave emission from a model coronal loop are shown in Fig. 1 (Holman, Brosius and Pfarr 1988—unpublished poster presentation). An isothermal 2.5×10^6 K plasma is confined to dipole magnetic field lines so that the magnetic field strength at the top of the loop is 435 Gauss, and the maximum field strength in the loop (at the footpoints) is 551 Gauss. The plasma is in hydrostatic equilibrium, with a density of 1.5×10^{10} cm^{-3} at the top of the loop. An isothermal external plasma with a temperature of 5×10^4 K and a density of 1×10^9 cm^{-3} at the height of the loop apex, also in hydrostatic equilibrium, has been included as well. The loop is about 50 Mm long, 10 Mm high, and has a circular cross section at the apex with a diameter of 4 Mm. The model was designed to be consistent with the observational results of Webb et al. (1987) at 1.45 GHz and 4.9 GHz. The figure shows total intensity brightness temperature maps of the loop at nine frequencies in the vicinity of 5 GHz. The radio frequency (in GHz) is given to the left of each frame, and the maximum brightness temperature (in millions of degrees K) is given on the right. The observer is at a location 60° above the plane of the photosphere, and 60° out of the plane of the loop (measured from the -x axis).

The model results demonstrate how observations over a small range of microwave frequencies can map out the structure of a coronal loop. At 4.8 GHz and 6.0 GHz, only optically thin thermal bremsstrahlung contributes to the emission. The entire loop is visible, but at low brightness temperatures. At 4.0 GHz and 4.4 GHz the third harmonic emission level cuts through the loop. Most of the loop is bright at 4.0 GHz because the harmonic level (where B = 475 Gauss) is contained within most of the upper part of the loop. The brightness temperature is somewhat less than the electron temperature because of absorption by the external plasma. At 4.4 GHz the harmonic level cuts through the "footpoints" of the loop. The asymmetry of the emission results from the viewing angle.

The emission from 4.85–5.6 GHz is 4th harmonic. The harmonic level again is lower in the loop at higher frequencies. The angular size of the 4th harmonic gyroresonance source, in arcseconds, is shown on the three center panels. This size variation with frequency can be used to deduce the quantitative loop geometry. The interesting structure at 5.4 GHz results from the harmonic level passing just below the lower boundary of the loop apex.

The microwave total flux (left panel) and peak brightness temperature (right panel) spectra in this frequency range are shown in Fig. 2. The two peaks are from the 3rd and 4th harmonic gyroresonance emission. The width of each peak is determined by the range of field strengths within the hot loop. Evidence for such "cyclotron line" emission has been presented by Willson (1985) and Lang et al. (1987).

A simpler loop model is obtained if the magnetic field is generated by a sub-photospheric line current, rather than a dipole. In this case the loop is semi-circular in shape, and surfaces of constant magnetic field strength extend along the entire length of the loop. Therefore, for this model gyroresonance radiation is emitted along the entire length of the loop whenever a harmonic is within the loop. Such a model is not generally consistent with observations (cf. Webb et al. 1987, Brosius et al. 1992).

The microwave emission from dipole loop models has been studied by Hol-

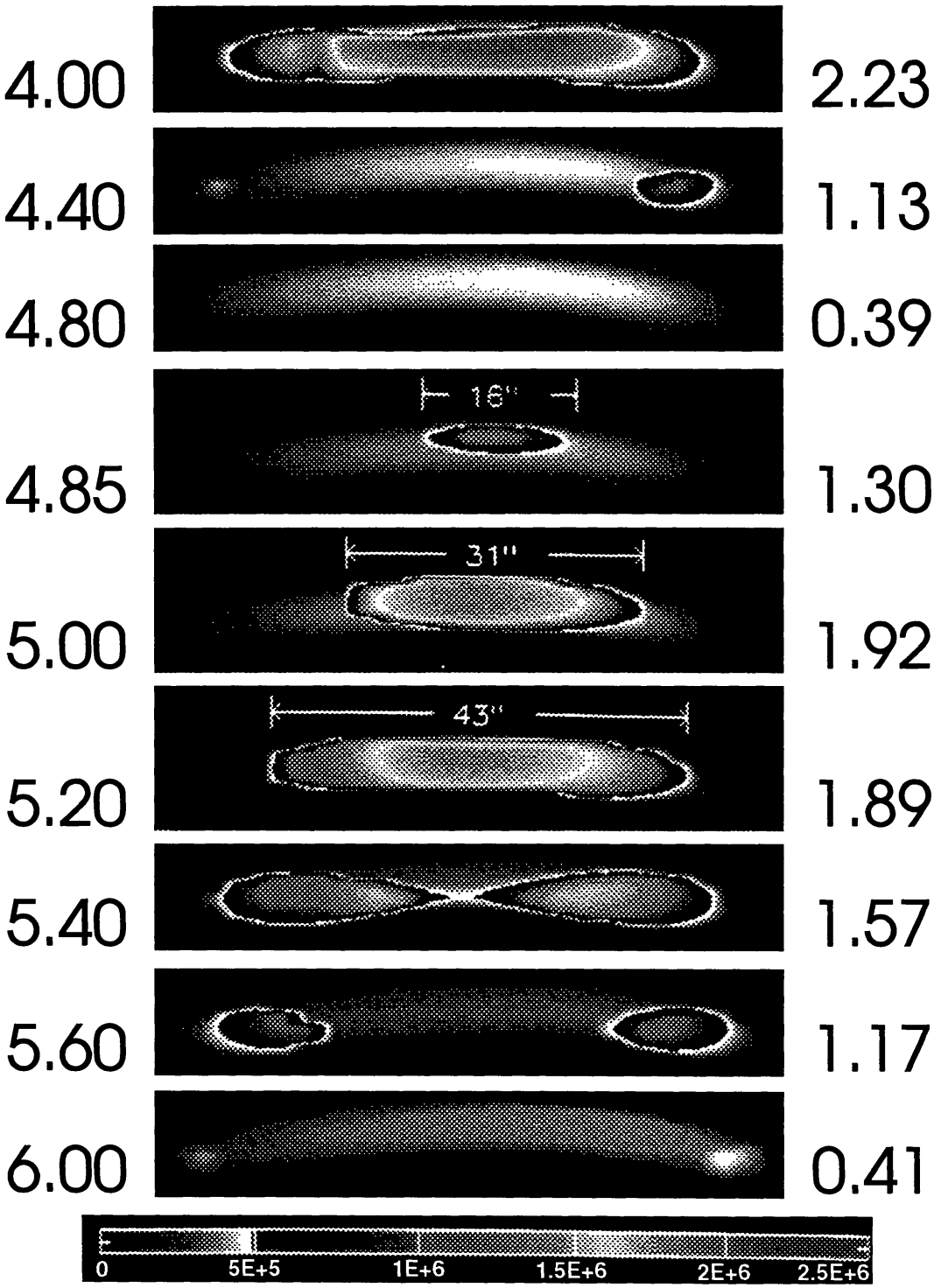

Figure 1. Total intensity brightness temperature maps of the microwave emission from a model dipole loop are shown. The radio frequency in GHz is shown to the left of each frame, and the peak brightness temperature ($\times 10^6$ K) is shown on the right.

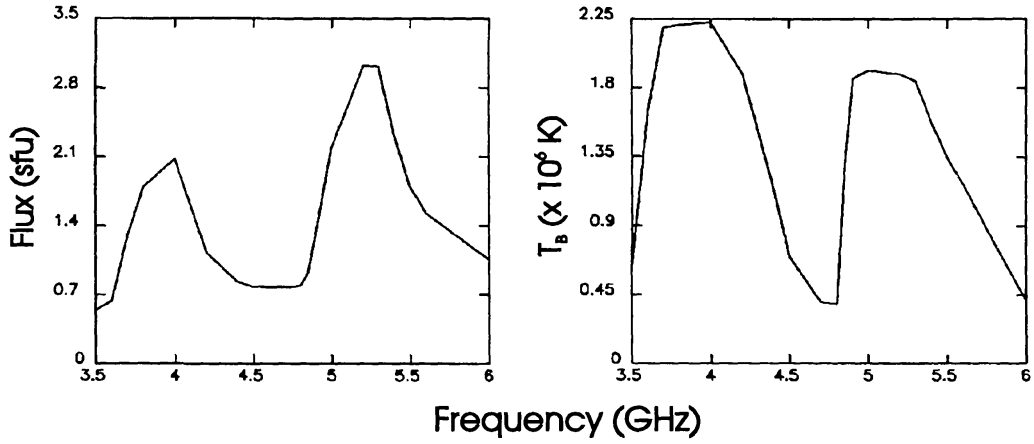

Figure 2. Total flux and peak brightness temperature spectra for the dipole loop model are shown. The microwave flux is in solar flux units (1 sfu = 10^{-19} erg cm^{-2} s^{-1} Hz^{-1}).

man and Kundu (1985). Models for the microwave emission from sunspots have been computed by Brosius and Holman (1989) and authors referenced therein. Such models provide the basis for the interpretation of microwave and coordinated observations of active region structures.

4. Applications to Active Region Data

Skylab, the Solar Maximum Mission (SMM), and flights of rocket-borne instruments, along with developments in radio astronomy instrumentation, provided the opportunity to obtain a better understanding of the relationship between the soft x-ray and radio emissions from the Sun. This in turn made it possible to develop our ability to obtain quantitative information from coordinated observations of these emissions. A review of these developments can be found in Strong et al. (1994). Specific examples are provided here.

4.1. Magnetic Field Strength from Gyroresonance Emission

The 1987 Coronal Magnetic Structures Observing Campaign (CoMStOC '87) was specifically designed to develop our ability to determine the magnetic field strength in the corona. Of the active regions observed during this campaign, the strongest fields were found in AR 4906 (S35E18), observed on December 18, the only region that contained a well developed sunspot (Brosius et al. 1992). The region was observed at 8 microwave frequencies with the VLA, 4 in the 20 cm band and 4 in the 6 cm band, and in soft x-rays with the SMM X-Ray Polychromator (XRP), as were all of the CoMStOC '87 regions. A longitudinal magnetogram was obtained from the Beijing Observatory.

Calculations of the microwave emission expected from the sunspot, using a dipole magnetic field model consistent with the measured photospheric field and a conventional model for the sunspot atmosphere, showed that the sunspot should be bright at both 6 and 20 cm. The brightest microwave emission from

the active region was associated with the sunspot, but the structure of the emission in both total intensity and polarization were not as expected. At 6 cm a compact, polarized source was observed over the sunspot. This source was shifted away from the center of the spot, however, toward a nearby region of opposite polarity. At 20 cm the peak emission was between the spot and the opposite polarity region. Hence, the bright microwave emission was found to be associated with a loop connecting the sunspot with a following region of opposite polarity, rather than with the overall sunspot field. The loop was also apparent in a potential field extrapolation of the photospheric magnetogram. The fact that the sunspot did not appear in microwaves as predicted, and no significant x-ray emission was present above the spot, indicated that the temperature and density were low above the sunspot.

No 6 cm emission was observed over the region of opposite polarity. Within the 20 cm band it was found that the peak of the emission was closer to the spot at higher frequencies. Therefore, the multifrequency microwave observations showed the loop to be highly asymmetric and provided a mapping of the magnetic field gradient within the structure. Our modeling of the polarization structure of the 6 cm emission and a consideration of the weak x-ray emission observed in this part of the active region led to the conclusion that the 6 cm radiation was third harmonic gyroresonance emission, requiring a magnetic field strength of 547-583 Gauss (this range of field strengths accounts for the range of frequencies at which observations were made in the 6 cm band). Fourth harmonic emission could be ruled out because, among other problems, the density required to reproduce the observed polarization structure was so high that the plasma frequency would be above 5 GHz, rendering the source invisible at this frequency. Second (and first) harmonic emission was ruled out because it required a plasma density that was several orders of magnitude lower than required for the weak x-ray emission observed from the location of the 6 cm source. Reproducing the polarization structure required that the density at the location of the 6 cm source be between 5×10^8 cm^{-3} and 2×10^9 cm^{-3}.

The 20 cm emission did not appear to be restricted to a single harmonic. Modeling and comparison with a potential field extrapolation of the photospheric magnetogram led us to conclude that the 20 cm emission was a combination of 2nd and 3rd harmonic gyroresonance radiation, yielding field strengths ranging from 160-300 Gauss in that part of the structure.

The magnetic field strengths deduced for this loop were consistent with the potential field extrapolation of the photospheric magnetogram. This was not the case in other parts of this active region, however (Brosius et al. 1992), or in other active regions where field strengths higher than the extrapolated values were required (e. g., Nitta et al. 1991, Schmelz et al. 1992).

As an example of the impact of these observations upon our understanding of the corona, we look at the implications of these results for coronal heating theory. The derived magnetic field strengths and emission measures give Alfven speeds ranging from 10 Mm s^{-1} to 40 Mm s^{-1} for the observed active region loop, significantly greater than the generally quoted value of 1–2 Mm s^{-1}. The corresponding range of values for the ratio of the electron gyrofrequency to the plasma frequency, an important quantity for studies of plasma wave processes in the corona, is ~1.5–6. Since in wave heating theories the heating rate is

proportional to the Alfven speed and the square of the wave velocity amplitude, these higher Alfven speeds allow the same heating rate to be achieved with a smaller wave amplitude. On the other hand, for the wave to be resonant with the loop, as in resonant absorption theories, the period of the driving wave must be shorter. For a loop length of 100 Mm and an Alfven speed of 20 Mm s^{-1}, the wave period must be 10 s or less.

A spectral method for determining the magnetic field strength at the base of the corona using gyroresonance emission is now available from the Owens Valley Radio Observatory. Gary and Hurford (1993) use the microwave spectral shape to distinguish gyroresonance emission from thermal bremsstrahlung. Since the (optically thick) brightness temperature spectra follow the temperature of the solar atmosphere, and higher frequencies generally correspond to lower heights in the atmosphere, the spectra turn over at a frequency corresponding to the top of the transition region (e. g., Zheleznyakov 1970). Assuming third harmonic emission, the frequency at which this drop to lower brightness temperatures occurs gives the magnetic field strength at the bottom of the corona (see equation 5). Gary and Hurford (1993) were able to obtain reliable spectra over an active region with a spatial resolution of 16 arcseconds. From this they could produce a "coronal magnetogram" of the magnetic field strength at the base of the corona above this region.

4.2. Longitudinal Magnetic Field from Thermal Bremsstrahlung Polarization

A "longitudinal coronal magnetogram" for a plage region was obtained by Brosius et al. (1993) using thermal bremsstrahlung polarization measurements. The region (at N11W10) was observed by the VLA at 20 cm, and at EUV wavelengths with the NASA/Goddard Solar EUV Rocket Telescope and Spectrograph (SERTS). Intensity ratios of Fe XVI to Fe XV emission lines were used to determine the temperature (2.3–2.9 $\times$ 10^6 K) and emission measure throughout the region. These temperature and emission measure maps were then used to make a brightness temperature map of the predicted thermal bremsstrahlung from this coronal plasma at 20 cm.

The predicted and observed 20 cm total intensity brightness temperature maps were similar in structure. Using the revised Meyer (1991) coronal iron abundance, they also agreed quantitatively. The revised Meyer abundances associate hydrogen with high first ionization potential (FIP) rather than low FIP elements. The result is that iron is a factor 3.4 times more abundant relative to hydrogen than in the earlier Meyer (1985) abundances. The earlier abundances give predicted brightness temperatures that exceed the observed values. When predicted brightness temperatures significantly exceed observed brightness temperatures, one is generally led to conclude that cooler plasma must be present in the corona to partially absorb the emission from the hotter plasma and bring down the brightness temperature of the escaping radiation (e. g., Webb et al. 1987, Nitta et al. 1991, Schmelz et al. 1992, Brosius et al. 1992). The revised abundances reduce this discrepancy. For these observations the revised abundances were sufficient to remove the discrepancy, with the result that no cooler plasma is required. The conclusion, therefore, was that the 20 cm emission was thermal bremsstrahlung from the same plasma observed in Fe

XV and Fe XVI.

The coronal plasma was found to be optically thin at 20 cm and, therefore, the longitudinal magnetic field is well approximated by equation 4 (see also equation 7 of Brosius et al. 1993). The 20 cm polarization map was used to produce a map of the longitudinal magnetic field strength in the corona, giving values $\sim$ 30–60 Gauss in the microwave emitting region. This map was compared with potential field extrapolations to heights of 5 Mm and 10 Mm of a longitudinal magnetogram obtained with the NASA/NSO spectromagnetograph at Kitt Peak. The extrapolated and derived longitudinal field strengths were found to agree if the microwave polarization was generated within this height range.

4.3. Physical Parameters from Microwave Polarization Reversal

An additional method for obtaining information about the corona makes use of the sign of the microwave polarization. If the direction of the longitudinal component of the magnetic field reverses along the ray path of the radiation, so that the radiation passes through a layer where the magnetic field is transverse to the direction of propagation, the right-hand mode of polarization will change to left, and left to right, so that the physical modes (ordinary and extraordinary) remain unchanged. If the frequency of the radiation is high enough, however, the extraordinary and ordinary modes can strongly couple so that they invert and the handedness of the observed polarization remains unchanged. The condition for this coupling to occur is determined by the coupling coefficient (e. g., Zheleznyakov 1970)

$$C = 4.75 \times 10^{18} \frac{f_{GHz}^4}{n_e B^3} \left| \frac{d\theta}{ds} \right|, \tag{7}$$

where $|d\theta/ds|$ is the rate at which the angle of the magnetic field changes along the ray path (radians/cm), and the other parameters are defined as above (f is in GHz). If $C \gg 1$, the observed polarization does not change. If $C \ll 1$, the observed polarization is reversed (right$\leftrightarrow$left).

Schmelz et al. (1992) concluded from the analysis of their active region data that the observed polarization from part of the region must be inverted at 20 cm, but not at 6 cm. Analysis of the potential field extrapolation of a longitudinal magnetogram obtained with the Haleakala Stokes Polarimeter revealed the presence of the required transverse field region. We found (using the field extrapolation) that the peak microwave emission crossed this layer at a height $\sim$85 Mm. B ($\sim$ 6 Gauss) and $|d\theta/ds|$ could also be obtained from the potential field extrapolation. Requiring $C \ll 1$ at 20 cm, but $C \gg 1$ at 6 cm gave 1.8×10^7 cm$^{-3} \ll n_e \ll 1.3 \times 10^9$ cm^{-3}, or $n_e \approx 10^8$ cm^{-3} at this height above the photosphere.

This constraint on the coronal density required the use of a field extrapolation. An alternative approach would be to use a knowledge of the frequency at which $C \approx 1$ to determine B (see Gelfreikh 1991). This has the disadvantage that a model for the coronal density is required (unless an observational constraint on n_e can be obtained) and the value of $|d\theta/ds|$ must also be determined or assumed. On the other hand, the high power of B (B^3) softens the dependence of B on errors in these quantities.

5. Discussion

Progress in determining the physical properties and evolution of coronal structures depends upon the availability of well-calibrated instruments with good spatial and spectral resolution, as well as our ability to coordinate and ultimately co-align observations with these instruments, and to process and analyze large quantities of data from them. Significant progress can be made with relatively modest instrumentation. Strong support for the subsequent processing, analysis, and interpretation of these data is crucial, however. The co-analysis of these diverse data sets is necessary for obtaining an understanding of the complex coupling between photospheric and coronal phenomena, and provides insight and motivation for instrumental developments in each of the participating wavelength regimes.

Another Coronal Magnetic Structures Observing Campaign, CoMStOC '92, was held as part of the MAX '91 program. The campaign was centered around coordinated observations with the Yohkoh Soft X-ray Telescope (SXT), the VLA and Owens Valley Radio Observatory, and state of the art vector magnetographs, including high-resolution photospheric observations with Lockheed's Solar Optical Universal Polarimeter (SOUP). The higher spatial resolution of the SXT, improvements in the VLA observations, the spectral coverage of Owens Valley, and improvements in the photospheric observations distinguish this campaign from CoMStOC '87. These data are now available and contain a wealth of information about active region structures. The next major observational step is likely to be an extended campaign in coordination with SOHO (Holman 1992). In the meantime, coordinated ground-based observations with rocket flights of instruments that provide both spatial and spectral data for coronal structures are extremely valuable.

References

Brosius, J. W., Holman, G. D. 1989, ApJ, 342, 1172

Brosius, J. W., Willson, R. F., Holman, G. D., Schmelz, J. T. 1992, ApJ, 386, 347

Brosius, J. W., Davila, J. M., Thompson, W. T., Thomas, R. J., Holman, G. D., Gopalswamy, N., White, S. M., Kundu, M. R., Jones, H. P. 1993, ApJ, 411, 410

Gary, D. E., Hurford, G. J. 1987, ApJ, 317, 522

Gary, D. E., Hurford, G. J. 1993, ApJ, in press

Gelfreikh, G. B. 1991, Adv Space Res, 11, (1)89

Holman, G. D., Kundu, M. R. 1985, ApJ, 292, 291

Holman, G. D., Brosius, J. W., Pfarr, B. B. 1988, BAAS, 20, 713

Holman, G. D. 1992, in Proceedings of the First SOHO Workshop, ESA SP-348, 189

Lang, K. R., Willson, R. F., Smith, K. L., Strong, K. T. 1987, ApJ, 322, 1044

Meyer, J.-P. 1985, ApJS, 57, 173

Meyer, J.-P. 1991, Adv Space Res, 11, 269

Nitta, N., White, S. M., Kundu, M. R., Gopalswamy, N., Holman, G. D., Brosius, J. W., Schmelz, J. T., Saba, J. L. R., Strong, K. T. 1991, ApJ, 374, 374

Schmelz, J. T., Holman, G. D., Brosius, J. W., Gonzalez, R. D. 1992, ApJ, 399, 733

Strong, K. T., Haisch, B. M., Saba, J. L. R. 1994, The Many Faces of the Sun: Scientific Highlights from the Solar Maximum Mission, Springer-Verlag, in press

Webb, D. F., Holman, G. D., Davis, J. M., Kundu, M. R., Shevgaonkar, R. K. 1987, ApJ, 315, 716

Willson, R. F. 1985, ApJ, 298, 911

Zheleznyakov, V. V. 1970, Radio Emission of the Sun and Planets, Pergamon, Oxford

Group Discussion

Mikic: In your comment at the beginning of the talk you mentioned that "people claim that it is not possible to measure directly the coronal magnetic field", which you contest on the basis that radio observations allow you to deduce the coronal magnetic field. I think that most people will agree that radio observations give us the magnitude of the coronal magnetic field, but they do not give us the vector nature of the field. Thus it is not possible to deduce the topology of the coronal field and its connectivity, which is an important matter. I think the radio observations are very useful in conjunction with the force-free field estimation of coronal fields from vector magnetograms.

Holman: My comment was referring to blanket statements that there is no way to directly obtain information about the strength of the coronal magnetic field. It is true that microwave observations most directly give the scalar quantity B or $B_{||}$, not the vector field. There are ways to obtain the information about the vector field in the corona by computing the structure and polarization of the microwave emission at different frequencies and locations, but this is somewhat model dependent. I entirely agree that the best way to study coronal magnetic fields is with multi-wavelength (radio and x-ray and/or EUV) observations of the corona and photospheric vector magnetograms. It is very important to obtain these simultaneous observations and follow them up with the necessary data analysis, field extrapolations, and theoretical interpretation of the combined data

Fisher: I get the impression that finding the harmonic number for cyclotron radiation is a model dependent and ad-hoc procedure. Is there a systematic way of finding the harmonic number?

Holman: The harmonic number can generally be determined from the observed polarization of the emission and constraints on the density in the source. An example of this is given in my paper. When there is not enough information to determine the harmonic number, a lower limit on the field strength can be

obtained by assuming that the emission is the 4th harmonic. This field strength will generally be at most a factor of 2 smaller than the actual field strength.

Linker: The estimate of the field strength is linearly dependent on what you think the harmonic is. How well do you know of this?

Holman: See response to Fisher.

Judge: Are there technical and/or physical reasons why the radio wavelengths determination of properties of the coronal magnetic field may not be extended to the chromosphere and transition region?

Holman: The determination of the magnetic field strength can be extended into the transition region, usually with observations above 5 GHz. A practical limitation to this is that if there is high brightness temperature emission from the corona at these frequencies, the limited dynamic range of the observations may not allow the lower brightness temperature emission from the transition region to be observed.

Bastian: You compared the coronal magnetic field strengths inferred from 20 cm observations with those inferred from a potential field extrapolation, showing that they were in fairly good agreement at a height of 5 Mm. I would like to point out that Aschwanden and Bastian (1993) have performed stereo-scopic analysis of the 20 cm emission from solar active regions and show that the height of 20 cm sources is much greater than 5 Mm, the average being 25 Mm with a standard deviation of 15 Mm.

Holman: Since we did not know the height of the sources we studied, we took the inferred field strengths to be consistent with the extrapolations if they agreed with the extrapolated field strengths at heights between 5 Mm and 10Mm, or higher. If the microwave polarization of the sources we studied was generated at heights much greater that 5–10 Mm, then most of the field strengths we deduced do not agree with the extrapolations.